FEATURE

Magnetic Control of Plasma Current, Position, and Shape in Tokamaks

A survey of modeling and control approaches

by Giuseppe Ambrosino and Raffaele Albanese

Tokamaks are among the most promising devices for obtaining nuclear fusion energy from a high-temperature, ionized gas (plasma). The plasma in a tokamak is magnetically confined through electromagnetic fields generated by a set of poloidal field (PF) coils (see "Tutorial 1" in [1] for the definition of poloidal plane) distributed around the vacuum vessel (see Figures 1 and 2). Voltages applied to these coils drive currents that produce a magnetic field. This field changes the shape and position of the plasma and induces plasma current.

Future tokamaks are expected to be pulsed machines, with each pulse lasting tens of minutes. In each pulse, plasma is created, then ramped up to the reference flat-top current, heated to the ignition temperature (see "Tutorial 2" in [1]), maintained in a quiescent burning state, cooled down, and finally terminated. Although tokamaks have not yet reached burning conditions, initiation, current ramp-up, heating, flat-top, and ramp-down have been realized [1, Figure 7]. The time evolution of coil currents, along with the plasma geometrical and physical parameters that guarantee this sequence along a pulse, define a scenario (see "Tutorial 13" in [2]). A scenario is usually constructed from a finite number of plasma equilibria [3] computed by magnetohydrodynamics (MHD) (see "Tutorial 3" in [1]) equilibrium codes [4]–[9], which determine the plasma geometry and current density distribution in force balance with the magnetic field. Feedforward coil currents or voltages

1066-033X/05/$20.00©2005IEEE

are then determined to obtain the desired magnetic field [10]–[12].

Since the feedforward nominal coil voltages are based on an approximate plasma model, feedback control is necessary. Moreover, to maximize the performance-to-cost ratio, plasmas with vertically elongated cross sections have to be used (see "Tutorial 10" in [2]); this elongation, unfortunately, leads to instability of the plasma vertical movements [13], necessitating feedback stabilization. In addition, a strong motivation for improving plasma control in next-generation tokamaks is that the plasma boundary must be maintained as close as possible to nearby components (see "Tutorial 6" and "Tutorial 7" in [3]). This objective guarantees the best use of the available volume and helps to ensure passive stabilization by inducing mirror currents in the neighboring metallic structures, hereafter named *passive structures*. Hence, the ability to control the shape of the plasma while ensuring good clearance is an essential feature of the plasma control systems.

The plasma-circuit system, consisting of the plasma, the surrounding passive structures, and the external circuits, is a distributed parameter system whose dynamic behavior is described by a set of nonlinear partial differential equations (PDEs). To obtain an approximate low-order model, we introduce simplifying assumptions. Since the approximations depend on the plasma geometrical parameters, only a limited number of weakly coupled variables are generally controlled, as illustrated below. Typical controllers have a proportional-integral differential (PID) structure and are designed using simple models of the system and fine-tuned during tokamak operation. Recently, the stringent plasma boundary control requirements for the International Thermonuclear Experimental Reactor (ITER) project [14], [15] have motivated researchers to improve the modeling of plasma response as well as the design of feedback controllers.

Time Evolution of a Tokamak Plasma

A tokamak is comprised of three subsystems, namely, the plasma, control circuits, and passive conductors, which interact with each other through electromagnetic fields. The evolution of the system [16] is governed by Maxwell's equations in their quasi-stationary form, as presented in "Tutorial 15."

The design of plasma current, position, and shape controllers is generally based on the following simplifying assumptions.

Assumption 1: The plasma-circuit system in a tokamak is assumed to be axisymmetric. It has been shown [17], [18] that axisymmetric effects play a crucial role in elongated plasmas. The influence of the eddy currents (see "Tutorial 14") induced in three-dimensional structures by time-varying magnetic fields has been studied in [19] and [20], showing that their main effects on the plasma can be reproduced by introducing a set of equivalent axisymmetric circuits.

Assumption 2: When representing the electromagnetic interaction of the plasma with the surrounding passive

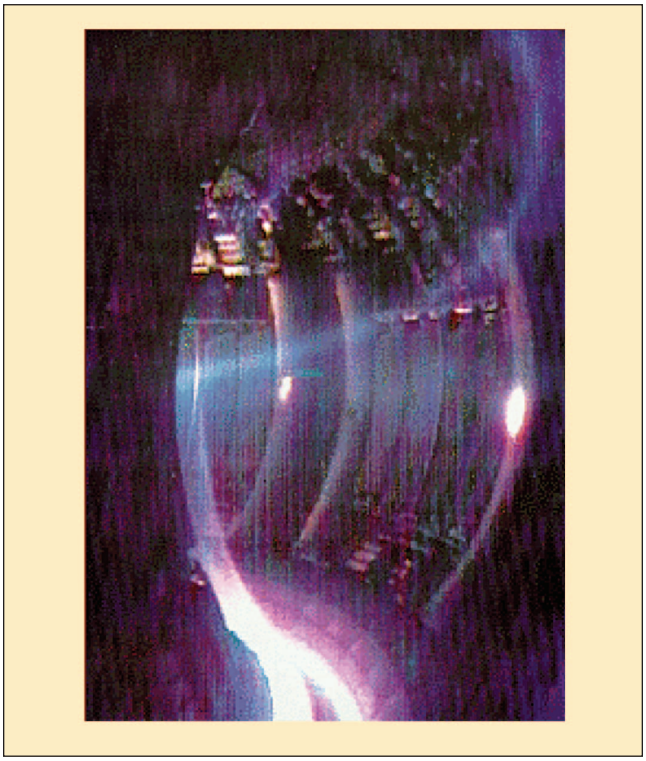

Figure 1. *Plasma in the JET tokamak situated at Culham, United Kingdom, during operation. The high-temperature plasma must not touch the vessel interior wall. To achieve this objective, the plasma column is confined through electromagnetic fields. (Photograph courtesy of EFDA-JET.)*

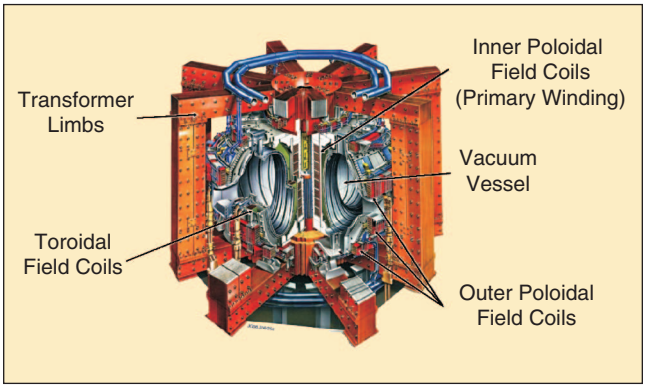

Figure 2. *Schematic drawing of the coil system in the JET tokamak. The electromagnetic fields that control plasma shape, position, and current are generated by the currents flowing in a set of PF coils distributed around the vacuum vessel. These currents are driven in feedback on the basis of measurements of the plasma position and boundary. (Courtesy of EFDA-JET.)*

Tutorial 14: Magnetic Fields, Currents, and Forces

Confinement and shaping of tokamak plasmas is made possible because of well-known relationships between magnetic fields, currents in conductors, and the forces that result from the interaction of the two. Figure A illustrates the so-called $J \times B$ forces produced by the cross product of a current density J and magnetic field B. Often, the symbol I is used to represent one or more lumped currents—in one or more wires, for example—while J is used to represent a continuous distribution of current or current density (current per unit area).

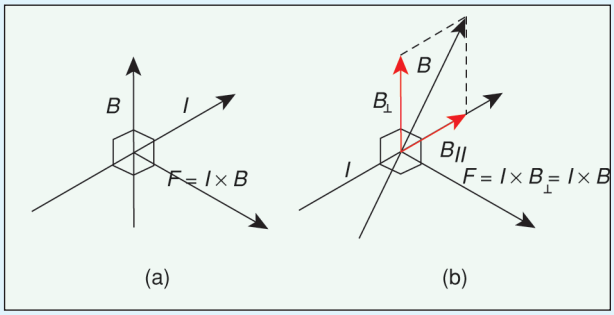

Figure A. *Illustration of magnetic force on a current-carrying conductor. The force per unit length exerted on a conductor carrying a current I by a magnetic field B is given by the cross product of I and B. The vectors I and B are shown orthogonal in (a). The more general case is shown in (b). Only the portion B⊥ of B orthogonal to the current I produces a force on that conductor.*

Since a tokamak plasma carries current, it can play the role of the conductor upon which magnetic fields can apply forces. For axisymmetric plasma shape control, the actuators are PF coils (see [1, Figure 4]) that carry only toroidal currents (in the direction of toroidal coordinate ϕ (see [1, Figure A of "Tutorial 1"]) and, therefore, generate only (axisymmetric) PFs. The forces on the plasma resulting from these PFs are dominated by their interaction with the plasma toroidal current density distribution J (Figure B). The resulting $J \times B$ forces are therefore directed poloidally. Thus the shape control problem may be considered by restricting to a poloidal (R, z) cross section (Figure B) of the device and plasma.

The vertical instability that must be stabilized when controlling the axisymmetric shape (see "Tutorial 12" in [2]) originates in the generation of a magnetic field used to improve the performance of the plasma. By vertically elongating the plasma, several performance parameters, including the toroidal β parameter (see "Tutorial 2" in [1]), can be increased. A circular plasma (Figure B) is vertically stable. To

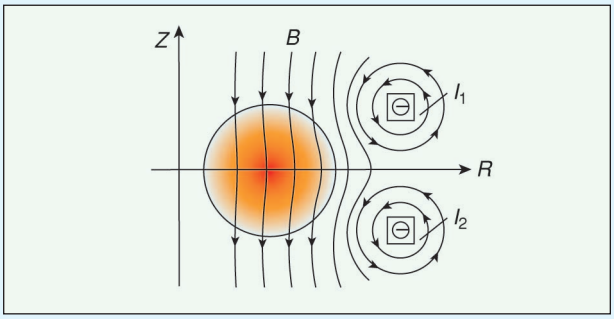

Figure B. *Illustration of radial force balance in plasmas. Plasmas exert a self-force known as the hoop force that is directed radially outward. The sign of the current in the outer coils is negative (coming out of the page) to produce magnetic field at the plasma that opposes this outward force and maintain the plasma position. The direction of magnetic field produced by a control coil is determined by the so-called right hand rule: If the thumb of the right hand indicates the direction of current, then the curled fingers of the right hand indicate the direction of the magnetic field produced by this current. The intensity of shading within the plasma is used to illustrate the continuous toroidal current density distribution j_ϕ (amps per square meter, for example) within the plasma. Since current is positively directed (into the page), the $J \times B$ force applied by the control coils is directed radially inward.*

structures and active coils, the plasma current profile (see "Tutorial 5" in [1] and "Tutorial 16") can be described by means of a finite number of global parameters. In [21] it is shown that the plasma current profile can be approximately represented by three degrees of freedom, namely, total plasma current I_p, poloidal beta β_{pol}, and internal inductance ℓ_i (see "Tutorial 12" in [2]). When this assumption holds, the gas state equation [(7) in "Tutorial 15"], which is used to derive the pressure profile, can be ignored.

Assumption 3: At the time scale of interest for current, position, and shape control, because of the low plasma mass density ρ, inertial effects can be neglected. Therefore, the plasma can be assumed to be in equilibrium at each time instant, and thus the terms on the left hand side of the momentum balance equation [(6) in "Tutorial 15"] can be neglected.

Assumption 4: Skin currents, which flow on the plasma boundary, can be neglected [22], [23].

make a vertically elongated plasma however, a radial magnetic field must be applied to pull upward on the top of the plasma and downward on the bottom of the plasma. The resulting magnetic field distribution (Figure C) is the source of the vertical instability. Under the influence of this field, upward (downward) displacements of the plasma result in a destabilizing upward (downward) force on the plasma.

Currents cannot only create magnetic fields and flux (see "Tutorial 1" in [1]) but can also be created by them. One simple example (see "Tutorial 12" in [2]) is the transformer action used to generate plasma current, in which changing flux, created by a subset of the set of PF coils, creates a loop voltage that drives current in the plasma.

Changing flux can also be produced by motion of the plasma. For example, when the plasma moves vertically, the magnetic flux due to the plasma current (see "Tutorial 1" in [1]) moves with the plasma. Therefore the poloidal flux value Ψ at a fixed toroidal conductor (a PF coil or a section of the conductive vacuum vessel, for example) changes as this flux distribution moves past it. The resultant loop voltage $V = -d\Psi/dt$ (see "Tutorial 12" in [2]) induces current according to $LdI/dt + RI = V$, where L and R are the inductance and resistance of the toroidal conductor. All toroidal conductors are affected by the plasma motion in a similar manner, inducing a collection of currents called *eddy currents*.

These induced eddy currents can have a net beneficial effect on plasma control. The magnetic fields produced by the eddy currents all produce forces on the plasma that act to oppose the continued motion, thereby acting as a mechanism for passive stabilization for the vertical instability. These currents are not sustained indefinitely, however, since the conductor resistance causes the current to decay, thereby reducing the associated magnetic field and its resultant force on the plasma. Thus, eddy currents cannot actually stabilize the instability but have a net effect of decreasing the growth rate (unstable eigenvalue) of the instability, making the combined plasma and conductors system less unstable. These eddy currents can also have a detrimental effect on plasma control, however, by shielding the magnetic fields produced by a PF coil and thus reducing its ability to affect a plasma on the other side of a conducting wall.

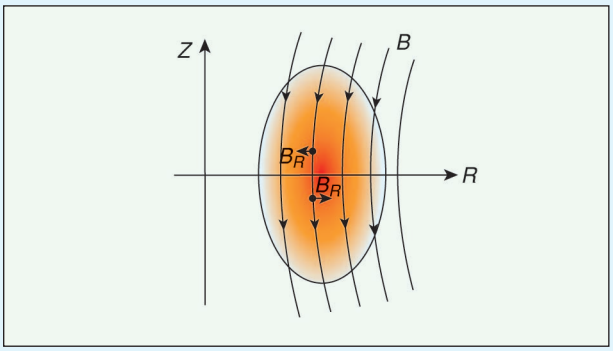

Figure C. *Illustration of the source of vertical instability. The magnetic field with radial component directed inward above the midplane and directed outward below the midplane is generated by the shaping coils to cause the plasma to become elongated. The $J \times B$ force for inward (outward) directed magnetic field and positive toroidal current (into the page) is up (down). As long as the current distribution and magnetic field are completely symmetric about the midplane ($z = 0$), the upward and downward forces balance, and the plasma is in equilibrium. If a disturbance shifts the plasma up slightly, more current will be above the midplane than below and the net force is directed upward. This imbalance causes the plasma to move up, thereby further increasing the upward force. A similar situation occurs if the disturbance causes an initial downward displacement of the plasma. This behavior is the essence of the vertical instability.*

During the last two decades, the validity of these assumptions has been confirmed by simulation and experiments, as discussed below.

Based on assumptions 1–4 and "Tutorial 15," the problem can be stated as the following PDE system governed by the operator Δ^* defined by [(11) in "Tutorial 15"] [10]:

- in the plasma region the Grad-Shafranov equation is given by

$$\Delta^*\psi = -f\frac{df}{d\psi} - \mu_0 r^2 \frac{dp}{d\psi}, \tag{1}$$

  where the sum of the two terms to the right of the equal sign represents the plasma toroidal current density
- in the coil and conductor region

$$\Delta^*\psi = -\mu_0 r\, j_{\text{ext}}(r, z, t), \tag{2}$$

where j_{ext} is the toroidal current density in the external conductors and coils

- elsewhere

$$\Delta^* \psi = 0, \tag{3}$$

with the initial and boundary conditions

$$\begin{aligned} &\psi(r, z, t) = \psi_0(r, z), \\ &\psi(0, z, t) = 0, \\ &\lim_{r^2+z^2\to\infty} \psi(r, z, t) = 0. \end{aligned} \tag{4}$$

Equations (1)–(4) are used to calculate the poloidal flux ψ function at time t provided that the plasma boundary can be determined, the current density j_{ext} is known, and the functions $p(\psi)$ and $f(\psi)$ are defined.

The plasma boundary (see "Tutorial 10" in [2]) is usually defined to be the outermost closed magnetic surface inside the vessel and is determined by an iterative calculation. In accordance with Assumption 2, the functions $p(\psi)$ and $f(\psi)$ can be expressed in terms of the plasma parameters I_p, β_{pol}, and ℓ_i. Therefore (1)–(4) is a free boundary problem, which, for each time t, gives the plasma equilibrium once the plasma parameters I_p, β_{pol}, and ℓ_i are fixed and the toroidal current density $j_{\text{ext}}(t)$ in the external conductors is assigned or dynamically calculated.

The toroidal current density $j_{\text{ext}}(t)$ can be expressed as a linear combination of the PF circuit currents. Therefore, the magnetic flux and the plasma configuration can be determined when prescribing the vector of currents $\boldsymbol{I}$ (including the PF currents and the plasma current I_p) along with β_{pol} and ℓ_i. The time evolution of these currents is given by the circuit equation

$$d\boldsymbol{\Psi}/dt + \boldsymbol{R}\,\boldsymbol{I} = \boldsymbol{U},$$

where $\boldsymbol{\Psi}$ is the vector of magnetic fluxes linked with the circuits, $\boldsymbol{R}$ is the resistance matrix, and $\boldsymbol{U}$ is the vector of applied voltages. The magnetic fluxes linked with the circuits depend on the magnetic configuration and therefore are functions of $\boldsymbol{I}$, β_{pol}, and ℓ_i (further details are given in "Derivation of Circuit Equations.")

Plasma Radial Position and Current Modeling and Control

The use of feedback for plasma position, current, and shape control has been extensively investigated in the last few decades. These control systems are used to maintain the plasma at a desired equilibrium configuration during the flat-top phase [1, Figure 7]. Controller design for these systems is usually based on low-order, linear, time-invariant models. The focus for investigators has been to introduce physical simplifying assumptions and use approximate numerical methods to obtain lumped parameter approximations of the PDE model (1)–(4).

To simplify plasma motion control, early tokamaks used sets of PF coils symmetrically placed with respect to the tokamak equatorial plane to guarantee mutually independent vertical and horizontal movement of the plasma. The problem is separated into two orthogonal parts: the horizontal position and current control by means of up-down symmetric currents and the vertical position control by means of up-down antisymmetric currents.

Initially, research efforts concentrated on the radial position control of circular, vertically stable tokamak plasmas. Rather than using the PDE equilibrium model (1)–(4), the radial dynamics can be modeled using the Shafranov lumped parameter equilibrium equation [24]. This equation gives the vertical field B_z required to maintain a plasma, having a major radius R and a minor radius a (Figure A in "Tutorial 1" in [1]), in radial equilibrium

$$B_z = B_z(R, I_P, a, \beta_{\text{pol}}, \ell_i) = \frac{\mu I_P}{4\pi R}\left[ln\frac{8R}{a} - \frac{3}{2} + \beta_{\text{pol}} + \frac{\ell_i}{2}\right]. \tag{5}$$

Although developed for large aspect ratio (R/a) circular cross-section plasmas, (5) has been shown to be accurate for small aspect ratios and noncircular plasmas, even with unusual toroidal current density [25].

The procedure given in [26] for obtaining a linearized model of the plasma-circuit dynamics based on (5) can be summarized as follows.

Step 1: Based on physical simplifying assumptions, functional dependencies of a, I_p, β_{pol}, and ℓ_i on the major radius R are established. These additional equations reduce the number of independent variables. A first assumption is toroidal flux conservation, which leads to the relation $a^2 \propto R$. Additional assumptions depend on the particular situation of the plasma. In [27], the authors consider the plasma heating phase and assume that $\beta_{\text{pol}} \propto R^{-7/3} I_p^{-2}$ from the adiabatic behavior of the plasma and $\ell_i/2 \propto R^{-2} I_p^{-2}$ from the invariance of safety factor q (see "Tutorial 4" in [1]). The result is that $B_z = B_z(R, I_p)$. In [29], independent variations of the parameter $\Lambda = \beta_{\text{pol}} + \ell_i/2$ are considered, in which case, the vertical field becomes $B_z = B_z(R, I_p, \Lambda)$.

Step 2: The vertical field B_z required to maintain the plasma in radial equilibrium is generated by the toroidal currents. Assuming a massless plasma, B_z has the simple form

$$B_z(R, I_p) = B_{\text{ext}}(R, \boldsymbol{I}), \tag{6}$$

where B_{ext} is the vertical field generated by the vector of currents $\boldsymbol{I}$, including the plasma current I_p, the active coil

Derivation of Circuit Equations

The relationship between the toroidal current density in the control circuits and the poloidal flux can be obtained from Faraday's law [(1) in "Tutorial 15"] and Ohm's law [(5) in "Tutorial 15"]. In principle, the active powered coils and the passive conductors can be treated in the same way. The only difference is in the applied voltage, which is zero in the passive conductors. It can be shown [16] that

$$j_{\text{ext}} = -\frac{\sigma}{r}\frac{\partial}{\partial t}\psi + \frac{\sigma}{2\pi r}u, \tag{1}$$

where u is the voltage applied to the coil ($u = 0$ for a passive conductor). Equation (1) must then be integrated over the coil and conductor regions. Using the standard loop current method for electrical circuits [70], the current density can be expanded as

$$j_{\text{ext}} = \sum_{k=1}^{n} I_k(t) J_{k\varphi}(r, z), \tag{2}$$

where n is the number of independent loop currents and $J_{k\varphi}$ is the toroidal component of the current density $\boldsymbol{J}_k$ associated with the kth loop current I_k. The n circuit equations in their standard form can be obtained by dividing both sides of (1) by σ, multiplying by the distribution $J_{k\varphi}$, and integrating over the conducting region V_c to obtain

$$\int_{V_C} J_{k\varphi}\sigma_{-1} j_{\text{ext}} dV = -\int_{V_C} J_{k\varphi}\frac{1}{r}\frac{\partial\psi}{\partial t}dV + \int_{V_C} J_{k\varphi}\frac{1}{2\pi r}u dV. \tag{3}$$

The integrals in (3) represent the resistive term, the inductive contribution, and the applied voltage, respectively. Equations (1)–(2) can also be used to account for the eddy currents induced in the metallic structures surrounding the plasma. In this case, expansion (2) provides only an approximation of the eddy-current distribution, which is acceptable provided that the deviation from axisymmetry is not dramatic.

Finally, three equations are needed to determine the time evolution of the plasma parameters I_p, β_{pol}, and ℓ_i. The parameters β_{pol} and ℓ_i are often viewed as disturbances, and their dynamics are prescribed on the basis of physical assumptions or experience gained with experimental activity. As for the plasma current, there are various modeling options. For instance, in the vertical position control problem (see "Tutorial 12" in [2]) the plasma current is assumed to be constant; for rapid transients the plasma current is assumed to vary so as to conserve the poloidal flux at the magnetic axis [1, Figure C in "Tutorial 1"], the average poloidal flux, or other integral quantities such as the helicity, which is related to a linkage of toroidal and poloidal magnetic fields, and is approximately conserved throughout a discharge, or the toroidal flux (see "Tutorial 1" in [1]). In some cases, the time evolution of the plasma current is derived from Ohm's law [(5) in "Tutorial 15"]. For instance, using a procedure similar to that used to obtain the circuit equations (3) [22] yields the scalar plasma current equation

$$\frac{1}{I_p}\int_{V_p} \boldsymbol{J}\cdot\sigma^{-1}\boldsymbol{J}\, dV = \frac{1}{I_p}\int_{V_p} \boldsymbol{J}\cdot(\boldsymbol{E} + \boldsymbol{v}\times\boldsymbol{B})\, dV. \tag{4}$$

Integration over the whole plasma volume V_p allows contributions of the plasma velocity to be incorporated along with poloidal components of the electric field in terms of the remaining unknowns [10]. In this way, (4) takes a form similar to (3).

currents ($I_1, \ldots, I_n$), and a vector $\boldsymbol{I_S}$ of currents accounting for the electromagnetic effects of the currents flowing in the passive structures.

Step 3: Circuit equation (2) is written in the form

$$d(\boldsymbol{LI})/dt + \boldsymbol{RI} = \boldsymbol{U}, \tag{7}$$

where $\boldsymbol{U}$ is the vector of voltages applied to the circuits (nonzero for the active coils), $\boldsymbol{R}$ is the circuit resistance matrix, and $\boldsymbol{L}$ is the matrix of self- and mutual inductances between the plasma, the coils, and the equivalent circuits of the passive structures [30], [31]. It should be noted that the inductance terms relating the plasma to fixed conductors are functions of the major radius R so that $\boldsymbol{L} = \boldsymbol{L}(R)$.

Step 4: For a fixed nominal vector of currents $\boldsymbol{I_0}$, which imply a nominal major radius R_0 and inductance matrix $\boldsymbol{L_0}$, derive the linearized model. This model can be obtained by differentiating (6) with respect to the major radius R to obtain dR/dt in terms of $d\boldsymbol{I}/dt$ as well as other free plasma parameters, such as β_{pol}, ℓ_i, or a linear combination. Substituting dR/dt in circuit equation (7), after standard manipulation, a linearized model can be obtained in the state-space form [32]

$$d\boldsymbol{x}/dt = \boldsymbol{Ax} + \boldsymbol{Bu} + \boldsymbol{E}d\boldsymbol{w}/dt,$$

where $\boldsymbol{x}$ is the vector of current deviations from nominal values, and $\boldsymbol{w}$ is the vector of $[\beta_p \cdot \ell_i]^T$ deviations. The vector $\boldsymbol{w}$ can be viewed as a disturbance vector.

Alternative lumped parameter approximations for obtaining a lumped parameter model of the passive structures have been studied. In [27] an accurate approximation of the vessel is obtained by using a finite element method. The order of the linearized model is reduced by means of a singular perturbation technique, where a low number of eddy-current time constants suffice to account for the vessel. In [29] an eigenmode description of the poloidal distribution of the toroidal currents is adopted; the first eigenmode provides a simple first-order description of the passive structure for analyzing the effect of the power supply dynamics on the plasma controllability.

Coupling between the plasma radial position and current control systems depends on the active poloidal coil system. In traditional tokamak designs, a decoupled system of poloidal windings is used. This system consists of an ohmic heating (OH) winding that controls the ohmic magnetic flux (see "Tutorial 9" in [3]) and thus the plasma current as well as a vertical field (VF) circuit that controls the plasma major radius according to (6). For these tokamaks, the simplest controller structure consists of two separate single-input, single-output (SISO) controllers. For more complex systems, or when high performance is required, multi-input, multi-output (MIMO) decoupling controllers are needed.

In [27], a linear quadratic (LQ) optimal controller for plasma radial position and current in the tokamak fusion test reactor of the Princeton Plasma Physics Laboratory during the flat-top phase is proposed. This controller computes the voltages of the OH and VF coils as a linear combination of eight measurements, namely, plasma radius and

Tutorial 15: Derivation of the Fundamental PDE and the Grad-Shafranov Equation

The dynamics of the quantities of interest for position and shape control in a tokamak are governed by quasi-stationary Maxwell's equations, given by

$$\nabla \times \boldsymbol{E} = -\frac{\partial \boldsymbol{B}}{\partial t}, \tag{1}$$

$$\nabla \times \boldsymbol{H} = \boldsymbol{J}, \tag{2}$$

$$\nabla \cdot \boldsymbol{B} = 0, \tag{3}$$

with the constitutive relationships

$$\boldsymbol{B} = \mu \boldsymbol{H}, \tag{4}$$

$$\boldsymbol{J} = \sigma(\boldsymbol{E} + \boldsymbol{v} \times \boldsymbol{B} + \boldsymbol{E}_i), \tag{5}$$

where $\boldsymbol{E}$ is the electric field, $\boldsymbol{B}$ is the magnetic flux density, t is the time, $\boldsymbol{H}$ is the magnetic field, $\boldsymbol{J}$ is the current density, μ is the magnetic permeability, σ is the electric conductivity, $\boldsymbol{v}$ is the velocity, and $\boldsymbol{E}_i$ is the impressed field, namely, the force per unit charge due to external sources.

Equation (1), where $\nabla\times$ is the curl operator, is Faraday's law of electromagnetic induction in its differential form. Equation (2) is Ampère's law, where the term related to the displacement current is neglected; with this assumption, valid for systems where the electric field does not vary too rapidly, the current density is divergence free. Equation (3), where $\nabla\cdot$ is the divergence operator, is Gauss's law for magnetism. Equations (4) and (5) express the material properties for a class of media that are present in a tokamak. In particular, (5) is Ohm's law in its local form.

In the plasma region, the Lorentz term $\boldsymbol{v} \times \boldsymbol{B}$ has an important effect. The plasma velocity is determined by the momentum balance

$$\rho\left(\frac{\partial \boldsymbol{v}}{\partial t} + \boldsymbol{v} \cdot \nabla \boldsymbol{v}\right) = \boldsymbol{J} \times \boldsymbol{B} - \nabla p, \tag{6}$$

where ∇ is the gradient operator and p is the kinetic pressure. Pressure, velocity, and density are coupled by thermodynamic and fluid equations. For a single, nondissipative fluid involving adiabatic behavior and entropy conservation, the thermodynamic equation has the form

$$\frac{\partial (p\rho^{-\gamma})}{\partial t} + \boldsymbol{v} \cdot \nabla (p\rho^{-\gamma}) = 0, \tag{7}$$

where ρ is the mass density and γ is the gas adiabatic exponent. Finally, mass conservation yields the continuity equation

$$\frac{\partial \rho}{\partial t} + \nabla \cdot (\rho \boldsymbol{v}) = 0. \tag{8}$$

In axisymmmetric geometry with cylindrical coordinates (r, ϕ, z), the vectors $\boldsymbol{B}$ and $\boldsymbol{J}$ can be expressed in terms of two scalar functions, namely, the poloidal magnetic flux and the poloidal current. The poloidal flux $\Psi(r, z)$ is the magnetic flux linked with the circumference obtained by revolving the point (r, z) around the z axis. The vertical component of $\boldsymbol{B}$ is then given by $B_z = (\partial\Psi/\partial r)/2\pi r$, as can

current, active coil currents, and their derivatives. In [28] this approach is extended to include the start-up phase in which the plasma shape expands and the plasma current increases so that the resulting model is time varying. Finally, control of the plasma major radius and current in the ISX-B tokamak with a 2×2 generalized proportional differential (PD) controller is investigated in [29].

The Vertical Position Control

The tokamaks constructed in the 1970s had a circular, vertically stable plasma poloidal section, so that there were no serious vertical position control problems. Since then, however, it has become clear that improved plasma parameters, specifically, a cubic gain in total beta and increased energy confinement time (see "Tutorial 2" in [1]), can be obtained using a vertically elongated cross section. The first experiments performed on tokamaks such as TOSCA [33] confirmed these theoretical predictions. Unfortunately, to obtain a vertically elongated plasma, the decay index of the vertical equilibrium field, defined as $n = -(R/B_z)(\partial B_z/\partial R)$, must be negative [34], causing a vertical axisymmetric MHD instability [35] on the Alfvén time scale (see "Tutorial 17"). Theoretically, these instabilities can be stabilized by surrounding the plasma with a superconductive wall [5]. Standard conductive walls with positive electrical resistance can only slow down the unstable mode to the time scale of the time constant L/R [36]. To stabilize the plasma on a longer time scale, an active feedback system is required [37].

A systematic investigation of techniques for active stabilization of elongated plasmas is given in [38]. The plasma circuital model, or, simply, circuit model, used for modeling the plasma-vessel-coils system, combines physical simplicity with the potential for a high degree of accuracy in

be verified by considering the differential magnetic flux $d\Psi = \Psi(r + dr, z) - \Psi(r, z)$. Rather than the poloidal flux, the poloidal flux per radian $\psi(r, z) = \Psi(r, z)/2\pi$ is more frequently used to simplify the expressions, yielding $B_z = (\partial\psi/\partial r)/r$. In addition, the divergence-free condition (3) yields the radial component $B_r = -(\partial\psi/\partial z)/r$, since the differential flux $d\Psi = \Psi(r, z + dz) - \Psi(r, z)$ is exactly balanced by the magnetic flux across the lateral cylindrical surface, where B_r is the normal component and dz is the height.

Using Ampère's law (2) and the constitutive equation (4), the total current linked with the circumference obtained by revolving (r, z) around the z axis is given by $I_{\text{pol}}(r, z) = 2\pi r B_\phi(r, z)/\mu(r, z)$. The poloidal current function $f = \mu I_{\text{pol}}/2\pi = rB_\phi$ is introduced to remove the coefficient $2\pi/\mu$. Therefore, the magnetic flux density can be expressed as

$$\boldsymbol{B} = \frac{1}{r}\nabla\psi \times \boldsymbol{i}_\phi + \frac{f}{r}\boldsymbol{i}_\phi, \tag{9}$$

where $\boldsymbol{i}_\phi$ is the unit vector in the toroidal direction (see "Tutorial 1" in [1]).

A similar expression can be derived for the current density

$$\mathbf{J} = \frac{1}{r}\nabla\left(\frac{f}{\mu}\right) \times \mathbf{i}_\phi - \frac{1}{\mu_0 r}\Delta^*\psi\ \mathbf{i}_\phi, \tag{10}$$

where μ_0 is the magnetic permeability of the vacuum, the poloidal components $J_r = -(\partial I_{\text{pol}}/\partial z)/2\pi r$ and $J_z = (\partial I_{\text{pol}}/\partial r)/2\pi r$ are expressed in terms of f, whereas the toroidal component is related to the second-order differential operator Δ^* defined by

$$\Delta^*\psi \equiv r\frac{\partial}{\partial r}\left(\frac{1}{\mu_r r}\frac{\partial\psi}{\partial r}\right) + \frac{\partial}{\partial z}\left(\frac{1}{\mu_r}\frac{\partial\psi}{\partial z}\right), \tag{11}$$

where $\mu_r = \mu/\mu_0$ is the relative magnetic permeability, which is unity in a vacuum and in nonmagnetic media such as air and plasma. Equation (11) is obtained from the toroidal component of Ampère's law (2) using the constitutive equation (4) and the magnetic flux expression (9) in terms of ψ.

At equilibrium, the plasma momentum balance (6) becomes $\boldsymbol{J} \times \boldsymbol{B} = \nabla p$, from which $\boldsymbol{J} \cdot \nabla p = 0$ and $\boldsymbol{B} \cdot \nabla p = 0$. In axisymmetric plasmas, taking into account expressions (9)–(10) and that $\mu = \mu_0$, these relationships yield $\nabla p \times \nabla\psi = \nabla p \times \nabla f = 0$. Hence $\nabla f \times \nabla\psi = 0$, and the equilibrium condition $\boldsymbol{J} \times \boldsymbol{B} = \nabla p$ becomes

$$-\mu_0\frac{\Delta^*\psi}{r^2}\nabla\psi - \frac{f}{\mu_0 r^2}\nabla f = \nabla p, \tag{12}$$

giving the Grad-Shafranov equation

$$\Delta^*\psi = -f\frac{df}{d\psi} - \mu_0 r^2\frac{dp}{d\psi}, \tag{13}$$

where Δ^* is defined by (11).

the external conductor and coils model. The plasma is modeled as a rigid wire loop free to move vertically. Neglecting the plasma mass, which plays a negligible role on the control time scale [39], the plasma vertical motions are described by a lumped parameter model.

To describe the plasma circuital model, let z denote the plasma vertical displacement, and let F' denote the z-derivative of the destabilizing force. The destabilizing force F' is the vertical force produced by the equilibrium field on a plasma subjected to a unit vertical displacement. Moreover, let $\boldsymbol{f}$ be the vector of the vertical forces acting on the plasma, produced by unit currents flowing in the circuits, and let $\boldsymbol{I}$ denote the vector of currents flowing in the passive and active circuits. With this notation, the force balance in the vertical direction is given by

$$F'z + \boldsymbol{f}^{\boldsymbol{T}}\,\boldsymbol{I} = 0. \tag{8}$$

Since the input to the system is the vector $\boldsymbol{U}$ of coil voltages, where the voltages applied to the passive circuits equal to zero, the circuit equation

$$d(\boldsymbol{LI})/dt + \boldsymbol{RI} + \boldsymbol{g}dz/dt = \boldsymbol{U} \tag{9}$$

must be combined with (8). In (9), $\boldsymbol{L}$ is the circuit inductance matrix, where $L_{jk} = \partial\Psi_j/\partial I_k$ is the contribution to the magnetic flux Ψ_j linked with the jth circuit, induced by a unit current I_k flowing in the kth circuit; $\boldsymbol{R}$ is the circuit resistance matrix; $\boldsymbol{g} = I_p\partial\boldsymbol{M}_{cp}/\partial z$, where I_p is the nominal plasma current; and $\boldsymbol{M}_{cp}$ is the circuit-to-plasma mutual inductance vector. The vector $\boldsymbol{g}$, where $g_j = \partial\Psi_j/\partial z$, gives the contributions to the magnetic fluxes linked with the circuits and induced by a unit displacement of the plasma.

For a rigid model, in which the plasma is modeled as a set of filaments free to move vertically while maintaining constant currents and relative positions, F' and $\boldsymbol{f}$ are given by

$$\boldsymbol{f} = \boldsymbol{g} = I_p\partial\boldsymbol{M}_{cp}/\partial z, \tag{10}$$

$$F' = 2\pi n B_z I_p. \tag{11}$$

The model (8)–(11) is used in [40] to analyze a feedback system consisting of a single passive coil and an active feedback coil. It is proved that proportional feedback of the plasma vertical position can stabilize the system, provided that the shielding effect of the passive coil, measured by the mutual inductance, is sufficiently small. However, this result is not quantitatively extendable to a massive structure of passive conductors. To overcome this difficulty, an eigenmode expansion of the vessel current is suggested in [39], where only the first eigenmode is retained. Using this approximation, a simple third-order model of the system is obtained. Moreover, using this model, a threshold value of the decay index can be calculated; above this value, derivative action is needed to stabilize the system.

The circuit model (8)–(11) has been used to design sophisticated controllers for plasma vertical stabilization. In [41] a modified LQ approach, which accounts for the time delay of the power supply, enlarges the n-index stability region with respect to the standard PD controllers. In [42] an H_∞ approach is used to design a vertical controller with low sensitivity to changes in the operating point. A low-order controller is also designed in [42] by using a reduced-order plant model obtained from balanced truncation. In [43], a predictive control algorithm is implemented on the COMPASS-D tokamak. This algorithm stabilizes the plasma using only flux sensors external to the vacuum vessel, as opposed to a standard PD controller, which uses mode estimates based at least partially on magnetic field sensors internal to the vacuum system. In [44], variable structure control for vertical stabilization of a tokamak plasma is able to handle edge-localized mode (ELM) disturbances (a form of plasma instability localized to the plasma edge) ("Tutorial 19" in the April 2006 issue) that are larger than those recovered by PD controllers. In [45], a derivative controller is used to stabilize the plasma vertical velocity. The derivative gain is adaptively changed with the growth time of the unstable mode: the variations of the growth time are detected by measuring the frequency of the plasma vertical oscillations around the equilibrium due to a deadzone in the power supply.

The weakness of the single-filament circuit model with a rigidly moving plasma is that this approach does not account for plasma shape deformations, which involve modified force equilibria. In particular, this model accounts for only the equilibrium field gradient at the chosen nominal location for the plasma filament. In [29] and [34], the plasma is represented as an array of fixed current-carrying filaments. In [38], it is shown that a single filament can produce growth rates and control properties that are significantly more optimistic than those obtained with a more realistic multifilament model. An MHD equilibrium code is used to choose the minimum number and positions of the plasma filaments.

The multifilament model, however, does not eliminate the main problem of the circuit approach, namely, that the plasma is modeled as a rigid body with a single degree of freedom (vertical displacement). In fact, the multifilament model can impose only one global constraint, namely the total vertical force balance, and does not guarantee local equilibrium of the forces. In [46], a linearized, nonrigid model of the plasma vertical displacements is presented. Equilibrium of the forces inside the plasma, described by Grad-Shafranov (1), is obtained by applying an MHD equilibrium code to the equilibrium (2) to calculate a modified inductance matrix L^*. For the rigid model,

Tutorial 16: Profiles

A number of relationships between plasma profiles ("Tutorial 5" in [1]) are used in the articles of this special section. The safety factor (q) profile was defined in "Tutorial 5" in [1]. An alternate definition is given by

$$q(\rho) = \oint \frac{1}{R}\frac{B\phi}{B_p} ds,$$

where B_ϕ is the toroidal field (TF) (field in the direction of the toroidal coordinate ϕ; see Figure A in "Tutorial 1" in [1]), B_p is the PF [field in the (R,Z) plane orthogonal to the coordinate ϕ], and the integration is carried out over a single poloidal circuit around the flux surface corresponding to the normalized flux value ρ ("Tutorial 5" in [1]) [71]. This definition illustrates why q is considered a measure of magnetic pitch. The TF B_ϕ is dominated by the contribution from the TF coils [1, Figure 4]), which are typically operated so as to produce an approximately constant (in time) TF. Thus, in most experiments, the safety factor profile is considered to be primarily a function (in time) of the variable poloidal component of the magnetic field. The PF B_p is produced by toroidal currents, including the current in the plasma and current in the PF coils. When the plasma shape is controlled at a steady-state equilibrium, the PF coil currents are nearly constant, so changes in PF are dominated by changes in the spatial distribution of plasma toroidal current density (the current profile). Through this chain of dependencies, it can be seen that the safety factor profile depends on the current profile (and vice versa). Thus, many physicists speak interchangeably of control of the current profile and of the q-profile.

A quantity known as the local *magnetic shear* is proportional to the spatial derivative of the safety factor, $s(\rho) \propto dq/d\rho$. Magnetic shear plays a role in plasma stability, but in the articles of this special section (and in much of the literature) it is used simply as an alternative description for the behavior of the q-profile. In particular, the notion of negative (central) shear, also known as *reverse shear*, describes a q-profile that is not monotonic (see the figure below). Another quantity related to q is the inverse of the safety factor known as iota, $t(\rho) = 2\pi/q(\rho)$. It can be shown that $t(\rho)$ is proportional to the total current inside the flux surface represented by the normalized flux value ρ. In particular, this means that the value $q(1) = 1/t(1)$ at the edge of the plasma is inversely proportional to the total plasma current. The q-, s-, and iota-profiles, are all functions of normalized flux ρ, while the current profile is not. The current profile is typically defined as the plasma current density along a line extending radially from the magnetic axis to the plasma edge (see "Tutorial 5" in [1]).

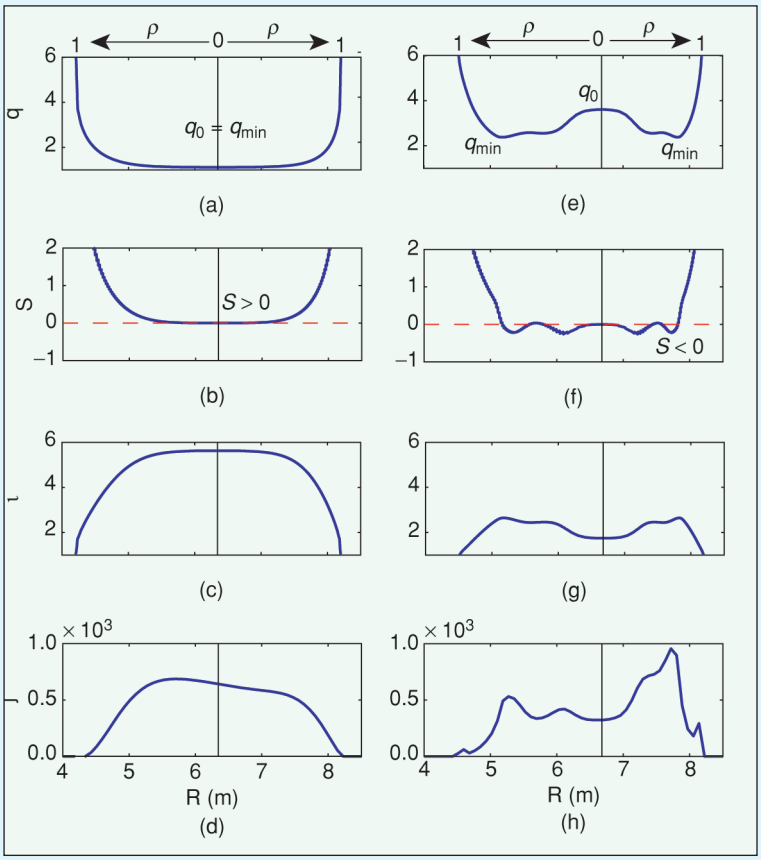

Examples of monotonic and reverse shear plasmas. Plots (a)–(d) represent the same plasma having a monotonic q-profile (in which q is monotonically increasing on $0 \le \rho \le 1$). Plots (e)–(h) represent a reverse shear plasma. [The normalized radius $x = r/a$ ("Tutorial 5" in [1]), although not identical to ρ, may be substituted for ρ everywhere in this figure and its description.] The vertical line in each plot indicates the radial location of the plasma magnetic axis ($\rho = 0$; see [1, Figure C in "Tutorial 1"]). A monotonic q profile (a) achieves its minimum value q_{min} at the magnetic axis $\rho = 0$ and is monotonically increasing in $0 \le \rho \le 1$. A reverse shear q profile (e) achieves its minimum value at $\rho > 0$, away from the magnetic axis. In either case, the value of q at the magnetic axis is denoted by $q_0 = q(\rho = 0)$. (b) The sign of the magnetic shear s for a monotonic q-profile is positive for all $0 \le \rho \le 1$. (f) A reverse shear plasma is one in which $s < 0$ for some set of values of ρ between zero and one. In particular, $s < 0$ near the magnetic axis, hence the name negative central shear. The quantity iota $t = 2\pi r/q$ is shown in plots (c) and (g). The current profile [(d), (h)] is not a function of the normalized flux coordinate ρ and so does not exhibit the same symmetry with respect to magnetic axis as the other quantities. The portion of the curve to the right of the magnetic axis in plots of q, s, and t appears compressed. This compression occurs because the plasma flux contours (see [1, Figure C in "Tutorial 1"]) are always spaced more closely near the outside of the torus, hence the radial dimension corresponding to the normalized flux $0 \le \rho \le 1$ must be smaller on that side of the magnetic axis.

(3) in "Derivation of Circuit Equations" can be rewritten [using (8) and (9)] as

$$\boldsymbol{L}^* d\boldsymbol{I}/dt + \boldsymbol{R}\boldsymbol{I} = \boldsymbol{U}, \tag{12}$$

where

$$\boldsymbol{L}^* = \boldsymbol{L} - (F')^{-1}\boldsymbol{g}\boldsymbol{f}^{\boldsymbol{T}}. \tag{13}$$

Expression (13) for $\boldsymbol{L}^*$ can be generalized to deformable plasmas. The terms $\boldsymbol{L}^*_{\boldsymbol{jk}}$, which are equal to $\partial\psi_j/\partial I_k$ in the presence of the plasma, can be determined, in the form of finite differences, by means of an MHD equilibrium code, which calculates the poloidal fluxes ψ_j at the nominal equilibrium, as well as at a perturbed equilibrium for small variations of the coil currents. When passing from the nominal to the perturbed equilibrium, the magnetic flux conservation assumption is suggested. The resulting numerical model, which is more accurate than the multifilament models, can be used for open-loop analysis and for designing stabilizing controllers. Furthermore, this model addresses the problem of optimal sensor location for reconstructing the plasma position and shape for deformable plasmas, as illustrated in [18], and for designing active stabilization systems for highly elongated plasmas [47].

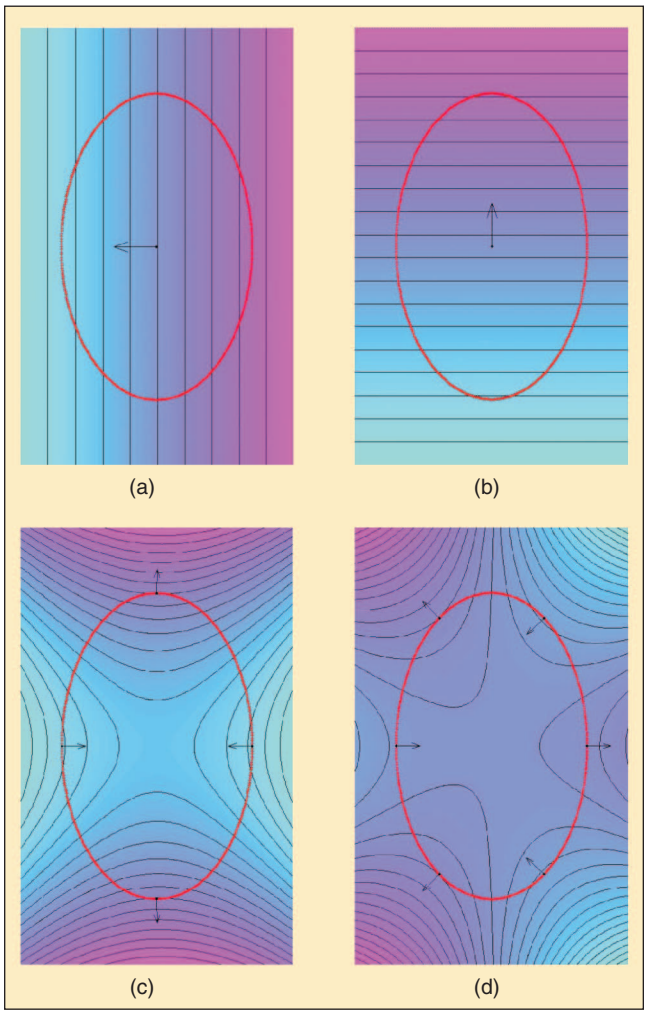

Figure 3. *The field lines and effects of multipolar fields on the plasma shape and position. The plasma is shown conceptually as an ellipse. The directions of the forces of field on the plasma are indicated by arrows. These forces are defined by $J \times B$, where J is the plasma current density and B is the magnetic field. (a) The effects of a vertical field, which mainly influences the radial position; (b) the effects of a radial field, which acts on the vertical position; (c) the effects of a quadrupole field, which mainly influences the plasma elongation; (d) the effects of an hexapole field, which determines the plasma triangularity.*

A modification of the linearization procedure illustrated in [46] is proposed in [48] to include the effect of the vessel on plasma stability. This model is obtained by approximating the plasma response to currents in the vacuum vessel in terms of equivalent PF coil currents. The linearized perturbed equilibrium plasma response model is used in [38] to study the stability of Alcator C-Mod equilibria. The growth rates of this model differ by up to a factor of 2 from those calculated using a rigid model. Additionally, the linear model was used for designing a vertical stabilization controller based on full-state-feedback pole placement combined with an observer that uses flux and field measurements and their calculated time derivatives.

Position, Current, and Shape Control

To make the best use of the available volume and to ensure good passive stabilization in large, highly elongated tokamaks, the plasma must be maintained as close as possible to nearby components such as the first wall, limiter, and baffles (see "Tutorial 6" and "Tutorial 7" in [3]). Thus, in addition to robust vertical stabilization control and efficient plasma current control, accurate shape control must be guaranteed. A further complication is that, due to engineering and maintenance constraints, the PF coil positions are not solely determined by magnetic decoupling considerations. Since it is not always possible to have separate coil sets for ohmic heating, vertical field, radial field, and shaping field, the resulting input-output model is highly coupled, and the control system must decouple among the controlled parameters.

We now consider three approaches to plasma shape control, namely, shape global parameter control, magnetic flux control, and gap control.

Shape Global Parameter Control Approaches

When a completely coupled position, current, and shape control problem is addressed, the first step is to model the coupled system using ordinary differential equations (ODEs) to approximate the PDE model. This model depends on the choice of the output variables to be controlled.

Initial efforts [49] were limited to controlling the plasma current, the radial and vertical position of the current centroid, and a few global shape parameters, for example, elongation κ and triangularity δ (see "Tutorial 10" in [2]). In [49] a conceptual tokamak is used as a reference example; the plasma current is modeled as a single filament located at the magnetic axis, with a shape defined by the elongation κ and the triangularity δ, calculated as a function of (R, a, β_{pol}, ℓ_i) using a semiempirical formula. The mutual inductances between the plasma and other circuits are determined using the filament approximation for the plasma, while the plasma self-inductance is calculated as a function of the full plasma dimensions (R, a, κ) and the internal inductance ℓ_i. The plasma filament is assumed to move instantaneously in response to a magnetic field present at its center to reach the new equilibrium. Finally, the equilibrium of the plasma, described by the parameters (R, a, κ, δ), is determined using a multipole representation of the externally applied poloidal magnetic field (see Figure 3). The vertical field B_z, the radial field B_R, the quadrupole field B_Q, and the hexapole field B_H required to maintain the plasma at the equilibrium are expressed as functions of (R, a, κ, δ, β_{pol}, ℓ_i, I_p). The equilibrium value of B_z is given by the modified Shafranov expression (5), which accounts for elongated cross sections and high poloidal beta; the radial field B_R is zero at the plasma filament location to ensure that vertical forces balance with the assumed symmetric plasma; B_Q and B_H are approximated by polynomial expressions whose coefficients are determined by fitting several plasma equilibria calculated using an equilibrium code. These four nonlinear algebraic equations, together with the toroidal flux conservation equation ($a^2 \propto R$ as specified in the section on plasma

Tutorial 17: Tokamak Time Scales

The various processes in tokamak plasmas evolve on a number of distinctively different characteristic time scales. These time scales range from less than a microsecond to many seconds. The fastest is the so-called Alfvén time scale, which refers to the growth time of those MHD ("Tutorial 3" in [1]) instabilities that have no passive stabilizing effects (the Alfvén instabilities or Alfvén eigenmodes). This time scale is also referred to as the ideal MHD time scale and the instabilities as ideal MHD instabilities. For example, the vertical displacement instability of a vertically elongated plasma ("Tutorial 12" in [2]) would have a growth time of a few microseconds or less were it not for the stabilizing influence of induced eddy currents in passive conducting structures (see "Tutorial 14"). When partially stabilized by induced currents in passive conductors, ideal MHD instabilities are converted to instabilities that grow on a time scale determined by the time needed for the induced currents to decay away due to conductor resistance. This time scale is sometimes called the wall time or resistive wall time. On present-day devices, the wall time is usually on the order of a few milliseconds but can vary considerably since it is determined by the resistance and inductance of the conducting elements in the device.

Other important time scales include the times required for evolution of transport quantities (density, temperature, and pressure profiles) and for evolution of the current profile (see "Tutorial 16"). In general, the current profile requires a much longer time to evolve (on the order of five or ten times greater) than the transport quantities. Characteristic time scales are often known by more than one label, which can be confusing. For example, transport time scales are also known as *confinement time scales*. Terms used for several similar current profile evolution characteristic times include the (global) resistive diffusion time, current diffusion time, skin time, and current relaxation time, the multiple names reflecting different characterizations of the physical processes that define the evolution. Although there are a number of other tokamak process time scales, those described above are the most relevant to the discussions in this special section.

The issue of characteristic time scale is important for tokamak control. For example, an unstable process with a fast time scale stresses the importance of fast real-time control calculations and actions. The requirement for fast response is the reason that control of the relatively fast and low dimensional plasma vertical instability is usually performed separately from the slower, high-dimensional plasma boundary shape control.

Control experiments must also run for a length of time sufficient to judge the effectiveness of new control methods. A primary goal of almost all tokamak control is the maintenance of some performance objective in steady-state conditions. The precise length of time that defines a steady-state evaluation is not universally agreed upon, but it clearly must have a length equivalent to multiple characteristic times of the process under control. As more control integration takes place, a significant challenge is to combine controls operating on the many different time scales.

radial position control), are used to calculate R, Z, a, κ, and δ for given values of $\beta_{\rm pol}$, ℓ_i, and I_p. To obtain a linearized model of the plasma-circuit dynamics based on these plasma equilibrium equations, a procedure similar to the one proposed in [27], and illustrated in the section on plasma radial position control, is used. As for the controller, [50] develops an LQ controller and discusses the choice of weighting matrices in the cost functional to account for control accuracy and voltage limitations. Moreover, model reduction is discussed, and a Kalman filter is used to estimate the eddy currents.

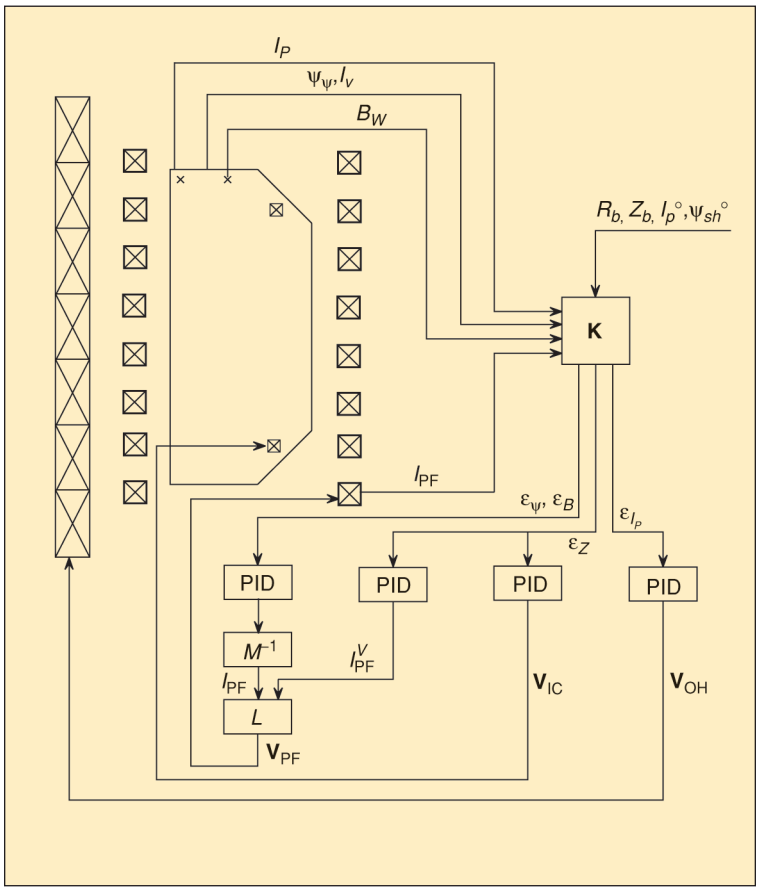

Figure 4. *Schematic representation of the control algorithm proposed in [51]. The feedback scheme consists of four basic components. The first component uses the matrix* $\boldsymbol{K}$ *to calculate the magnetic flux and field error signals as linear combinations of current, flux, and field sensor measurements as well as preprogrammed functions. The second component consists of a bank of PID controllers, one for each error signal. The error* ε_{I_p} *in the plasma current is used to define the voltage* $\boldsymbol{V}_{\rm OH}$ *of the ohmic heating coil; the error* ε_z *in the vertical position is used to define voltages* $\boldsymbol{V}_{\rm IC}$ *of the internal control coils; the errors* ε_ψ *and* ε_B *in the magnetic fluxes and fields are used to define voltages* $\boldsymbol{V}_{\rm PF}$ *of the external PF-shaping coils. The third component consists of the block labeled* M^{-1}*, which calculates the PF coil current derivatives needed to reduce the magnetic flux and field errors to zero in a fixed time interval* Δt*. The last element, labeled L, calculates, by means of the PF circuit equations, the PF coil voltage commands as a function of the coil currents, their time derivatives, and the loop voltage produced by the ohmic heating transformer.*

Magnetic Flux Control Approaches

In practice, controlling a few shape geometrical parameters cannot guarantee a high level of plasma shape accuracy. For example, in next generation tokamaks such as the ITER tokamak, the plasma-wall distance must be carefully controlled during the entire burn phase with an accuracy of a few centimeters to avoid contact of the hot plasma with the first wall. Alternatively [51], to control the plasma boundary, the poloidal flux and the poloidal magnetic field can be controlled at specified points. The coordinates of these points are preprogrammed along with the desired evolution of the plasma boundary. This control algorithm does not require preprogrammed currents, thus avoiding the need for preprogrammed current calculation. The feedback scheme (Figure 4) consists of four basic elements. The first element involves calculating the magnetic flux and magnetic field error signals as linear combinations of current, flux, and field sensor measurements, specified by a linear mapping matrix $\boldsymbol{K}$. The second element consists of a bank of PID controllers, one for each error signal, which calculate the voltage needed to reduce these errors to zero. The third element, labeled $\rm M^{-1}$, calculates the PF coil current derivatives needed to reduce the magnetic flux and field errors to zero in a fixed time interval Δt. To carry out this calculation, the vessel currents and the plasma effects are both neglected. The last element, labeled L, consists of a block that calculates, by means of the PF circuit equations, the PF coil voltage commands as a function of the coil currents, their time derivatives, and the loop voltage produced by the OH transformer. Since this control algorithm does not consider the plasma, the algorithm can be used during the entire scenario, but cannot guarantee high dynamic decoupling among the controlled variables. This algorithm is used in [52] to carry out simulation studies for the Korea Superconducting Tokamak Advanced Research (KSTAR) tokamak, while modified versions are in current use on some tokamaks, such as Alcator C-Mod [53] and TCV [54], which have powerful computers for real-time calculations.

Gap Control Approaches

To obtain better performance during the flat-top phase, a finite number of distances (gaps) between the first wall and the plasma boundary serve as regulated shape geometrical descriptors

[55]–[56]. In [57] this approach is used to design the shape controller for the JET tokamak located at Culham, United Kingdom. Although the plasma-circuit modeling and the controller design are based on several simplifying assumptions, the resulting shape controller has been shown to be flexible and adequate for many experimental tests [58]. In this approach, the vertical motion is stabilized by a velocity feedback controller, and the design of the shape controller is carried out neglecting the effect of the eddy currents, which is a valid assumption when the time scale of the shape control is longer than the decay times of the vessel currents. The plasma-coil dynamics are described by two lumped, nonlinear equations of the form

$$\boldsymbol{Y} = \boldsymbol{Y}(\boldsymbol{I}, \beta_{\text{pol}}, \ell_i, \psi_{\text{iron}}),$$
$$d(\boldsymbol{L}(\boldsymbol{Y}, \beta_{\text{pol}}, \ell_i, \psi_{\text{iron}})\boldsymbol{I})/dt + \boldsymbol{R}\boldsymbol{I} = U,$$

where $\boldsymbol{Y}$ is the vector of gaps, $\boldsymbol{I} = (\boldsymbol{I}_{\text{coils}}, I_p)$, and ψ_{iron} represents the iron core (see Figure 2) saturation status. A numerical procedure is used to obtain a linear model in a state space form having $\boldsymbol{U}$ as inputs, $\boldsymbol{I}_{\text{coils}}$ as state variables, and $\boldsymbol{Y}$ as outputs. The matrices of this model, which contains several derivatives of the vector $\boldsymbol{Y}$ and the matrix $\boldsymbol{L}$, are calculated using the equilibrium code PROTEUS [11]. In particular, the derivatives of the mutual inductances with respect to the gaps are approximated by replacing the plasma current with four filaments and calculating the derivatives with respect to radial and vertical movements of the filaments. Finally, the shape controller consists of a static matrix gain designed to decouple the gaps and assign closed-loop eigenvalues.

The linearized mathematical model consisting of the plasma equilibrium algebraic equations and the circuit differential equations is the basis of the procedure proposed

Tutorial 18: Plasma Disruptions

Disruptions are rapid events in which a large fraction of the plasma thermal energy is lost due to the uncontrolled growth of some large-scale plasma instability. These large-scale instabilities take place over a large portion of the plasma cross section. In most cases disruptions are unrecoverable (major disruptions), expelling nearly 100% of the thermal energy and leading to complete termination of the plasma current. More rarely, disruptive instabilities can fail to expel all of the thermal energy and may even allow the discharge to recover (a minor disruption). Two broad classes of events account for the vast majority of plasma-terminating disruptions in tokamaks: major disruptions and vertical displacement events (VDEs). VDEs are unique to plasmas that are intrinsically unstable to vertical displacements (the vertical instability; see "Tutorial 12" in [2]). This instability exists only in plasmas that are sufficiently vertically elongated (have cross sections that are higher than they are wide). A VDE is characterized by a loss of vertical position control, which allows the vertical instability to grow. The resulting vertical drift causes the plasma to strike a nearby surface, which erodes away the plasma as it continues to move into the wall. This erosion eventually destabilizes a large-scale instability, which expels all of the thermal energy. Following this thermal quench the plasma is always too cold and resistive for the ohmic transformer ("Tutorial 9" in [3]) to sustain the plasma current, which decays away and terminates the plasma. By contrast, a major disruption is characterized by a sudden thermal quench triggered by a large-scale instability before any loss of position occurs. In this case, the plasma becomes cold and resistive when more or less centered in the tokamak, and much of the plasma current can decay away before any subsequent loss of position causes the plasma to strike the wall.

Disruptions are undesirable in reactors due to a host of potentially damaging effects. The thermal quench can apply a large heat load to the first wall or divertor ("Tutorial 6" in [3]), possibly melting protective surfaces. Large currents can be driven by the disruption in both plasma-facing components and conducting structures, resulting in potentially damaging electromagnetic forces. The very high voltages produced in the cold postthermal quench plasma can accelerate electrons into a relativistic beam. This million electron volt (MeV) scale electron beam can destroy many types of plasma-facing components as the field lines they travel on intercept the first wall, much as an electron beam lithograph can etch features into semiconductor substrates.

Fortunately, many of these damaging disruption effects can be mitigated by taking corrective action as a stability limit is being approached or even after the disruption is underway. Furthermore, understanding of the instabilities whose growth lead to disruptions has advanced to the point that many of these disruptive stability limits are predictable. However, it remains a challenge to be able to predict an impending disruption in real time early enough and with sufficient reliability to execute the necessary corrective or mitigating action.

in [22] for obtaining the CREATE-L model of the plasma-circuit dynamics. Using spatial discretization of the active and passive circuits to integrate the PDE, viewing the plasma as a deformable superconductor, and using (1)–(4) to express the poloidal flux ψ in terms of I, I_p, $\beta_{\rm pol}$ and ℓ_i, a spatially discretized approximation of the PDE is given by the implicit state-space form

$$f(\boldsymbol{I}, d\boldsymbol{I}/dt, \boldsymbol{U}, \boldsymbol{W}, \boldsymbol{d}\,\boldsymbol{W}/dt) = 0,$$
$$\boldsymbol{Y} = \eta(\boldsymbol{I}, \boldsymbol{W}),$$

where the vector $\boldsymbol{I}$ of active and passive currents is the state vector, $\boldsymbol{Y}$ is the output vector including all the variables of interest (such as gaps, position of the current centroid, and other quantities to be monitored or controlled, including magnetic measurements), $\boldsymbol{U}$ is the vector of applied voltages, and $\boldsymbol{W} = [\beta_{\rm pol}, \ell_i]^T$ is viewed as a disturbance vector. Then, using a numerical approach based on the PROTEUS equilibrium code to calculate the derivatives of f and $\boldsymbol{Y}$, a linearized model about the nominal equilibrium in the standard state-space form is obtained. The resulting linearized model has been validated on experimental discharges of various fusion devices, including the TCV and JET tokamaks [59], [60].

The modeling approach developed in [22] was used to design an LQ plasma shape controller for ITER during the design phase [61]. It is shown in [62] that ITER plasma current and shape control issues, including power constraints, voltage limits, and plant uncertainties, can be cast in the H_∞ and μ-synthesis framework. Validation of these advanced design techniques has been carried out on the TCV tokamak [63]. This test, performed only during the flat-top phase, shows the superiority of these controllers in guaranteeing high performance, especially in terms of decoupling. Since these plasma-model-based controllers cannot operate with fixed parameters during the entire plasma discharge, it is necessary to develop switching controllers.

A modeling approach based on low poloidal mode number (see "Tutorial 4" in [1]) displacements of the plasma current distribution in [64] has been used to design shape controllers for DIII–D tokamak [65]. This controller, designed using normalized coprime factorizations, emphasizes X point (see "Tutorial 10" in [2]) control accuracy over shape accuracy. Successful experimental tests performed on several DIII–D discharges suggest the validity of the proposed modeling and design approach.

A more efficient model-based shape controller design approach [66], [67] considers extremely shaped plasmas in the JET tokamak, that is, plasmas with high triangularity and elongation. This approach seeks to control the entire plasma boundary rather than a small, fixed number of magnetic measurements (for example, magnetic fluxes) or plasma-wall gaps. The plasma is identified by a large number (up to 40) of geometrical descriptors [gaps plus X point and strike point positions (see "Tutorial 10" in [2])]. Finally, a singular value decomposition approach is used to optimize the control of the geometrical descriptors with the eight available coil currents (see [2] for details).

Conclusions

In this article, we reviewed plasma current, position, and shape control systems and modeling approaches. We divided the literature into three categories, namely, plasma radial position and current control, vertical stabilization of elongated plasmas, and plasma shape control.

The plasma current and radial position control problem can be easily solved using a filament plasma model, that is, the Shafranov lumped parameter equation (5) and two separate PID controllers. At most, a MIMO controller can be used if decoupling is desired.

Stabilization of the plasma vertical motion can be considered a solved problem. Recently, however, some researchers [68] have shown the possibility of errors in the estimation of the current centroid vertical position during vertical displacement events (VDEs) and plasma disruptions (see "Tutorial 18"), or in the presence of perturbations caused by ELMs [69]. These facts might require new control strategies in which the control algorithm is changed on the basis of an estimate of the measurement accuracy.

Several design approaches for shape control have been proposed in the literature. In the authors' opinion, controllers based on magnetic flux control [51] are useful for controlling the shape during the plasma formation and start-up phase, when the control requirements are not stringent. In contrast, high performance gap controllers [66] designed with accurate plasma-conductor models are expected to operate during the flat-top phase in future devices.

References

[1] A. Pironti and M. Walker, "Fusion, tokamaks, and plasma control," *IEEE Control Syst. Mag.,* vol. 25, no. 5, pp. 30–43, Oct. 2005.

[2] M. Ariola and A. Pironti, "Plasma shape control for the JET tokamak," *IEEE Control Syst. Mag.,* vol. 25, no. 5, pp. 65–75, Oct. 2005.

[3] A. Beghi and A. Cenedese, "Advances in real-time plasma boundary reconstruction," *IEEE Control Syst. Mag.,* vol. 25, no. 5, pp. 44–64, Oct. 2005.

[4] K. Lackner, "Computation of ideal MHD equilibria," *Comput. Phys. Commun.*, vol. 12, no. 1, pp. 33–44, Sept. 1976.

[5] J. Blum, J. Le Foll, and B. Thooris, "The self-consistent equilibrium and diffusion code SCED," *Comput. Phys. Commun.*, vol. 24, no. 3–4, pp. 235–254, Dec. 1981.

[6] S.C. Jardin, N. Pomphrey, and J. De Lucia, "Dynamic modeling of transport and positional control of tokamaks," *J. Comput. Phys.*, vol. 66, no. 5, pp. 481–507, May 1986.

[7] F. Hofmann, "FBT—A free boundary tokamak equilibrium code for highly elongated and shaped plasmas,'' *Comput. Phys. Commun.*, vol. 48, no. 2, pp. 207–221, Feb. 1988.

[8] R. Albanese, J. Blum, and O. De Barbieri, "Numerical studies of the next European torus via the PROTEUS Code,'' in *Proc. 12th Conf. Numerical Simulation of Plasmas*, S. Francisco, CA, 1987, paper IT4, pp. 1–2.

[9] R.H. Bulmer, "Tokamak physics experiment poloidal field design,'' in *Proc. 15th IEEE/NPSS Symp. Fusion Eng.*, Hyannis, MA, Oct. 1993, vol. 2, pp. 176–179.

[10] J. Blum, *Numerical Simulation and Optimal Control in Plasma Physics with Applications to Tokamaks*. New York: Wiley, 1985.

[11] R. Albanese, G. Ambrosino, R. Martone, and A. Pironti, "PF coil optimization for start-up scenarios in air core tokamaks,'' *IEEE Trans. Magn.*, vol. 30, no. 5, pp. 3423–3426, May 1994.

[12] R.D. Pillsbury and S.P. Hakkerainen, "Plasma startup modeling for ALCATOR C-MOD,'' in *Proc. 13th IEEE Symp. Fusion Engineering*, Knoxville, TE, Oct. 1989, vol. 1, pp. 642–645.

[13] K. Lackner and A.B. Macmahon, "Numerical study of displacement instability in elongated tokamak,'' *Nucl. Fusion*, vol. 14, no. 4, pp. 575–577, Sept. 1974.

[14] J. Wesley, H. W. Bartels, D. Boucher, A. Costley, L. De Kock, Y. Gribov, M. Huguet, G. Janeschitz, P.L. Mondino, V. Mukhovatov, A. Portone, M. Sugihara, and I. Yonekawa, "Plasma control requirements and concepts for ITER,'' *Fusion Technol.,* vol. 32, no. 3, pp. 495–470, Nov. 1997.

[15] A. Portone, R. Albanese, Y.V. Gribov, M. Huguet, D.H. Humphreys, C.E. Kessel, P.L. Mondino, L.D. Pearlstein, and J.C. Wesley, "Dynamic control of plasma position and shape in ITER,'' *Fusion Technol.,* vol. 32, no. 3, pp. 374–389, Nov. 1997.

[16] W.M. Stacey, *Fusion Plasma Analysis*. Melbourne, FL: Krieger, 1981.

[17] E. Rebhan, "Stability boundaries of tokamaks with respect to rigid displacements,'' *Nucl. Fusion*, vol. 15, no. 2, pp. 277–285, Apr. 1975.

[18] D.J. Ward and S.C. Jardin, "Effects of plasma deformability on the feedback stabilization of axisymmetric modes in tokamak plasmas,'' *Nucl. Fusion*, vol. 32, no. 6, pp. 973–993, June 1992.

[19] R. Albanese, R. Fresa, G. Rubinacci, and F. Villone, "Time evolution of tokamak plasmas in the presence of 3D conducting structures,'' *IEEE Trans. Magn.*, vol. 36, no. 4, pp. 1804–1807, July 2000.

[20] I. Senda, T. Shoji, T. Tsunematsu, T. Nishino, and H. Fujieda, "Approximation of eddy currents in three dimensional structures by toroidally symmetric models, and plasma control issues,'' *Nucl. Fusion*, vol. 37, no. 8, pp. 1129–1145, Aug. 1997.

[21] J.L. Luxon and B.B. Brown, "Magnetic analysis of non-circular cross-section tokamaks,'' *Nucl. Fusion*, vol. 22, no. 6, pp. 813–821, June 1982.

[22] R. Albanese and F. Villone, "The linearized CREATE-L plasma response model for the control of current, position and shape in tokamaks,'' *Nucl. Fusion*, vol. 38, no. 5, pp. 723–738, May 1998.

[23] H.G. Eriksson, "Axisymmetric stability of a toroidal pinch with non-circular cross-section,'' *Plasma Phys. Control. Fusion*, vol. 34, no. 12, pp. 1721–1748, Dec. 1992.

[24] V.D. Shafranov, "Plasma equilibrium in a magnetic field,'' *Revs. Plasma Phys.*, vol. 2, no. 1, pp. 103–151, Jan. 1966.

[25] H.D. Pacher, B.C. Gregory, and G.W. Pacher, "Magnetohydrodynamic equilibrium of tokamak plasmas with reversed current layers,'' *Nucl. Fusion*, vol. 26, no. 4, pp. 507–513, Apr. 1986.

[26] J. Hugill and A. Gibson, "Servo-control of plasma position in CLEO tokamak,'' *Nucl. Fusion*, vol. 14, no. 5, pp. 611–620, Nov. 1974.

[27] R. Gran, M.J. Rossi, and F. Sobierajski, "Plasma position control for TFTR using modern control theory,'' in *Proc. 7th Symp. Eng. Probs. Fusion Research*, Knoxville, TN, 1977, pp. 104–111.

[28] M.A. Firestone, "Analysis of modern optimal control theory applied to plasma position and current control in TFTR,'' *IEEE Trans. Plasma Sci.*, vol. 10, no. 2, pp. 105–115, June 1982.

[29] G.H. Neilson, G.R. Dyer, and P.H. Edmonds, "A model for coupled plasma current and position feedback control in the ISX-B tokamak,'' *Nucl. Fusion*, vol. 24, no. 10, pp. 1291–1302, Oct. 1984.

[30] Y. Nagayama, M. Naito, Y. Ueda, Y. Ohki, and K. Miyamoto, "Feedback control of vertical plasma position in non-circular tokamak TNT-A," *Nucl. Fusion*, vol. 24, no. 10, pp. 1243–1249, Oct. 1984.

[31] E.A. Lazarus and G.H. Neilson, "Solutions to the tokamak circuit equations with force balance for a massless plasma,'' *Nucl. Fusion*, vol. 27, no. 3, pp. 383–396, Mar. 1987.

[32] G. Ambrosino, G. Celentano, V. Coccorese, and F. Garofalo, "Controller design for plasma position and current control in NET,'' in *Proc. 15th Symp. Fusion Technology*, Utrecht, 1988, pp. 1670–1674.

[33] D.C. Robinson and A.J. Wootton, "An experimental study of tokamak plasmas with vertically elongated cross-sections,'' *Nucl. Fusion*, vol. 18, no. 11, pp. 1555–1567, Nov. 1978.

[34] M. Mori, N. Suzuki, T. Shoji, I. Yanagisawa, T. Tani, and Y. Matsuzaki, "Stability limit of feedback control of vertical plasma position in the JFT-2M tokamak," *Nucl. Fusion*, vol. 27, no. 5, pp. 725–734, May 1987.

[35] M. Okabayashi and G. Sheffield, "Vertical stability of elongated tokamaks,'' *Nucl. Fusion*, vol. 14, no. 2, pp. 263–265, Apr. 1974.

[36] D. Berger, L.C. Bernard, R. Gruber, and F. Troyon, "Numerical MHD stability calculation of a D-shaped, elongated, small aspect ratio tokamak,'' in *Proc. 8th Conf. Controlled Fusion Plasma Physics*, Prague, 1977, Paper 52, p. 52.

[37] E. Rebhan and A. Salat, "Feedback stabilization of axisymmetric MHD instabilities in tokamaks,'' *Nucl. Fusion*, vol. 18, no. 10, pp. 1431–1444, Oct. 1978.

[38] D.A. Humphreys and I.H. Hutchinson, "Filament-circuit model analysis of Alcator C-Mod vertical stability,'' Massachusetts Inst. Technol., Cambridge, MA, Int. Rep. PFC/JA-89_28, 1989.

[39] E.A. Lazarus, J.B. Lister, and G.H. Neilson, "Control of the vertical instability in tokamaks," *Nucl. Fusion*, vol. 30, no. 1, pp. 111–141, Jan. 1990.

[40] S.C. Jardin and D.A. Larrabee, "Feedback stabilization of rigid axisymmetric modes in tokamaks,'' *Nucl. Fusion*, vol. 22, no. 8, pp. 1095–1098, Aug. 1982.

[41] S. Moriyama, K. Nakamura, Y. Nakamura, and S. Itoh, "Analysis of optimal feedaback control of vertical plasma position in a tokamak system,'' *Jpn. J. Appl. Phys.*, vol. 24, no. 7, pp. 849–855, 1985.

[42] M.M.M. Al-Husari, B. Hendel, I.M. Jaimoukha, E.M. Kasenally, D.J.N. Limebeer, and A. Portone, "Vertical stabilization of tokamak plasmas,'' in *Proc. 30th IEEE CDC*, Brighton, UK, 1991, pp. 1165–1170.

[43] J.R. Gossner, P. Vyas, B. Kouvaritakis, and A.W. Morris, "Application of cautious stable predictive control to vertical positioning in COMPASS-D tokamak,'' *IEEE Trans. Contr. Syst. Technol.*, vol. 7, no. 5, pp. 580–587, Sept. 1999.

[44] L. Scibile and B. Kouvaritakis, "A discrete adaptive near-time optimum control for the plasma vertical position in a tokamak,'' *IEEE Trans. Contr. Syst. Technol.*, vol. 9, no. 1, pp. 148–162, Jan. 2001.

[45] M. Lennholm, D. Campbell, F. Milani, S. Puppin, F. Sartori, and B. Tubbing, "Plasma vertical stabilisation at JET using adaptive gain adjustment,'' in *Proc. 17th IEEE/NPSS Symp. Fusion Engineering*, San Diego, CA, 1997, vol. 1, pp. 539–542.

[46] R. Albanese, E. Coccorese, and G. Rubinacci, "Plasma modeling for the control of vertical instabilities,'' *Nucl. Fusion*, vol. 29, no. 6, pp. 1013–1023, June 1989.

[47] D.J. Ward and F. Hofmann, "Active feedback stabilization of axisymmetric modes in highly elongated tokamak plasmas," *Nucl. Fusion*, vol. 34, no. 3, pp. 401–415, Mar. 1994.

[48] D.A. Humphreys and I.H. Hutchinson, "Axisymmetric magnetic control design in tokamaks using perturbed plasma equilibrium response modeling," *Fusion Technol.*, vol. 23, no. 2, pp. 167–184, Mar. 1993.

[49] C.E. Kessel and M.A. Firestone, "Determination of gross plasma equilibrium from magnetic multipoles,'' *Fusion Technol.*, vol. 10, pp. 1177–1122, Nov. 1986.

[50] C.E. Kessel, M.A. Firestone, and R.W. Conn, "Linear optimal control of tokamak fusion devices," *Fusion Technol.*, vol. 17, no. 3, pp. 391–411, May 1990.

[51] F. Hofmann and S.C. Jardin, "Plasma shape and position control in highly elongated tokamaks,'' *Nucl. Fusion*, vol. 30, no. 10, pp. 2013–2022, Oct. 1990.

[52] H. Jhang, C.E. Kessel, N. Pomphrey, J.Y. Kim, S.C. Jardin, and G.S. Lee, "Simulation studies of plasma identification and control in Korea Superconducting Tokamak Advanced Research,'' *Fusion Eng. Des.*, vol. 54, no. 1, pp. 117–134, Feb. 2001.

[53] I.H. Hutchinson, S.F. Horne, G. Tinios, S.W. Wolfe, and R.S. Granetz, "Plasma shape control: A general approach and its application to Alcator C-Mod,'' *Fusion Technol.*, vol. 30, no. 2, pp. 137–150, Nov. 1996.

[54] J.B. Lister, F. Hofmann, J.M. Moret, F. Buhlmann, M.J. Dutch, D. Fasel, A. Favre, P.F. Isoz, B. Marletaz, P. Marmillod, Y. Martin, A. Perez, and D.J. Ward, "The control of tokamak configuration variable plasmas,'' *Fusion Technol.*, vol. 32, no. 3, pp. 321–373, Nov. 1997.

[55] S. Kinoshita, H. Fukumoto, A.G. Kellman, N. Hosogane, T. Osborne, E.J. Strait, and T.S. Taylor, "Independent control of gaps in single-null divertor discharge on the DIII-D tokamak,'' General Atomics, San Diego, CA, Int. Rep. GA-A19584, 1990.

[56] A. Pironti and A. Portone, "Optimal choice of the geometrical descriptors for the control of the shape of a tokamak plasma,'' *Fusion Eng. Des.*, vol. 43, no. 2, pp. 115–127, Feb. 1998.

[57] M. Garribba, R. Litunovsky, P. Noll, and S. Puppin, "The new control scheme for the JET plasma position and current control system,'' in *Proc. 15th IEEE/NPSS Symp. Fusion Engineering*, Hyannis, MA, 1993, pp. 33–36.

[58] M. Garribba, M.L. Browne, D.J. Campbell, Z. Hudson, R. Litunovsky, V. Marchese, F. Milani, J. Mills, P. Noll, S. Puppin, F. Sartori, L. Scibile, A. Tanga, and I. Young, "First operational experience with the new plasma position and current control system of JET,'' in *Proc. 18th Symp. Fusion Technology*, Karlsruhe, Germany, 1994, pp. 747–750.

[59] F. Villone, P. Vyas, J.B. Lister, and R. Albanese, "Comparison of the CREATE-L plasma response model with TCV limited discharges,'' *Nucl. Fusion*, vol. 37, no. 10, pp. 1395–1410, Oct. 1997.

[60] R. Albanese, G. Calabrò, M. Mattei, and F. Villone, "Plasma Response Models for Current, Shape and Position Control in JET,'' *Fusion Eng. Des.*, vol. 66–68, pp. 715–718, Sept. 2003.

[61] R. Albanese, G. Ambrosino, E. Coccorese, F.C. Morabito, A. Pironti, G. Rubinacci, and S. Scala, "Plasma current, shape, and position control in ITER,'' *Fusion Technol.*, vol. 30, no. 2, pp. 167–183, Nov. 1996.

[62] G. Ambrosino, M. Ariola, Y. Mitrishkin, A. Pironti, and A. Portone, "Plasma current and shape control in tokamaks using H_∞ and μ-synthesis,'' in *Proc. 36th IEEE Conf. Decision Control*, San Diego, CA, 1997, pp. 3697–3702.

[63] M. Ariola, G. Ambrosino, J.B. Lister, A. Pironti, F. Villone, and P. Vyas, "A modern plasma controller tested on the TCV tokamak," *Fusion Technol.*, vol. 36, no. 2, pp. 126–138, Sep. 1999.

[64] D.A. Humphreys, J.A. Leuer, and M.L. Walker, "Minimal plasma response models for design of tokamak equilibrium controllers with high dynamic accuracy,'' *Bull. Amer. Phys. Soc.*, vol. 44, pp. 175–180, Nov. 1999.

[65] M.L. Walker, D.A. Humphreys, J.A. Leuer, J.R. Ferron, and B.G. Penaflor, "Implementation of model-based multivariable control on DIII-D,'' *Fusion Eng. Des.*, vol. 56, no. 7, pp. 727–731, Oct. 2001.

[66] G. Ambrosino, M. Ariola, A. Pironti, and F. Sartori, "A new shape controller for extremely shaped plasmas in JET,'' *Fusion Eng. Des.*, vol. 66–68, pp. 797–802, Sept. 2003.

[67] F. Crisanti, R. Albanese, G. Ambrosino, M. Ariola, J.B.L. Lister, M. Mattei, F. Milani, A. Pironti, F. Sartori, and F. Villone, "Upgrade of the present JET Shape and Vertical Stability Controller," *Fusion Eng. Des.*, vol. 66–68, pp. 803–807, Sept. 2003.

[68] R. Yoshino, J.K. Koga, and T. Takeda, "Sensor algorithms of the plasma vertical position to avoid a vertical displacement event during plasma-current quench on JT-60U,'' *Fusion Technol.*, vol. 30, no. 2, pp. 237–250, Nov. 1996.

[69] F. Hofmann, I. Furno, S. Gerasimov, Y. Martin, F. Milani, M.F.F. Nave, H. Reimerdes, F. Sartori, and O. Sauter, "Effect of ELMs on the measurement of vertical plasma position in TCV and JET,'' *Nucl. Fusion*, vol. 42, no. 1, pp. 59–65, Jan. 2002.

[70] L.O. Chua, C.A. Desoer, and E.S. Kuh, *Linear and Nonlinear Circuits*. New York: McGraw-Hill, 1989.

[71] J. Wesson, *Tokamaks*. Oxford, UK: Clarendon Press, 1997.

Giuseppe Ambrosino (ambrosin@unina.it) graduated magna cum laude and received a degree in electronic engineering in 1975 from the Università di Napoli. He spent two years of study and research at Politecnico di Milano (1977–1978). He was an associate professor of system theory and automatic control at the Università di Napoli (1979–1986). Since 1986, he has been a full professor of automatic control. His present research interests are in applications of control theory in fields such as aerospace, thermonuclear plasmas, and industrial automation. He has been involved in several international projects in the field of fusion such as NET, Ignitor, ITER, FTU, and JET. He can be contacted at Dipartimento di Informatica e Sistemistica, Via Claudio, 21-80125 Naples, Italy.

Raffaele Albanese graduated magna cum laude and received a degree in aeronautical engineering in 1982 from the Università di Napoli, Italy, where he received his Ph.D. in electrical engineering in 1987. He was a member of the NET Team in Germany (1983–1986). In 1986–1994, he was at the University Salerno, Italy. Since 1994 he has been a full professor of electrical engineering at the University Mediterranea di Reggio Calabria, where he served as chair of the DIMET Department and Dean of the Faculty of Engineering. He is also administrator and scientific consultant of the CREATE Consortium, Italy. His current research interests are in nuclear fusion, computational electromagnetics, and plasma engineering.